Heat Sealing of Semicrystalline Polymer Films. II. Effect of Melting Distribution on Heat-Sealing Behavior of Polyolefins

FERDINAND C. STEHLING and PRASADARAO MEKA*

Exxon Chemical Co., P.O. Box 5200, Baytown, Texas 77522-5200

SYNOPSIS

Heat sealing of films, i.e., formation of a joint between two films by placing them fleetingly between heated platens, was experimentally investigated for a variety of semicrystalline polyolefins, especially various polyethylenes, to determine how sealing temperature affected seal strength measured at room temperature. Seal strength as a function of sealing temperature, $SS(T)$, is closely related to the melting distribution of the polymer determined by DSC measurements, i.e., to the fraction of amorphous phase as a function of temperature, $f_a(T)$. Seal initiation temperature, the temperature at which a specific, low level of seal strength of polyethylene films is achieved, corresponds to the temperature at which the fraction of amorphous phase equals 77 ± 3%. At higher temperatures, $SS(T)$ increases approximately as $f_a(T)$ increases. At the final melting point of the polymer, i.e., when $f_a(T) = 1$, seal strength reaches an approximately constant value termed the plateau seal strength. The magnitude of the plateau seal strength is determined by the yield stress of the polymer film. Thus, the heat-sealing curve, $SS(T)$, for a polyethylene can be semiquantitatively predicted from the melting distribution and yield stress of the polymer.

INTRODUCTION

Sealing of polymer films by application of heat is widely used in the packaging industry to join films. Heat-sealing methods, process variables, seal testing, and seal properties have been reviewed by Dodin,[1,2] Theller,[3] and Stokes.[4] In the first of this series of papers concerning heat sealing, a finite element modeling technique was used to calculate the interfacial temperature as a function of time during the sealing of semicrystalline polymer films between heated platens.[5] An experimental technique for measuring rapidly changing interfacial temperatures between two films during sealing was also developed. Good agreement was obtained between calculated and experimentally measured interfacial temperatures. The effect of heat-sealing process variables (seal platen temperature, dwell time, and pressure) on seal properties (seal strength, seal elongation, and seal energy) of monolayer polyethylene films was also quantitatively determined.

It was shown that seal properties are determined primarily by the maximum temperature achieved at the interface during heat sealing.[1] At preferred platen temperature and dwell time operating conditions, the maximum interfacial temperature approaches the platen temperature to within a few degrees. A plot similar to the idealized one shown in Figure 1 is typically obtained when seal strength measured at room temperature is plotted against platen temperature during sealing.

Molecular processes postulated to occur during heat sealing of semicrystalline polymer films are schematically illustrated in Figure 2. The surface of a film is rough on a microscopic scale, and the films are initially in intimate, Van der Waals contact at only a small fraction of the apparent film-contact area. When heat is applied, melting of the crystalline polymer occurs, and the application of slight pressure causes increased molecular contact, or wetting, of the molten film surfaces. In commercial heat-sealing processes for films heat, is applied for a sec-

* To whom correspondence should be addressed.

Journal of Applied Polymer Science, Vol. 51, 105-119 (1994)
 CCC 0021-8995/94/010105-15

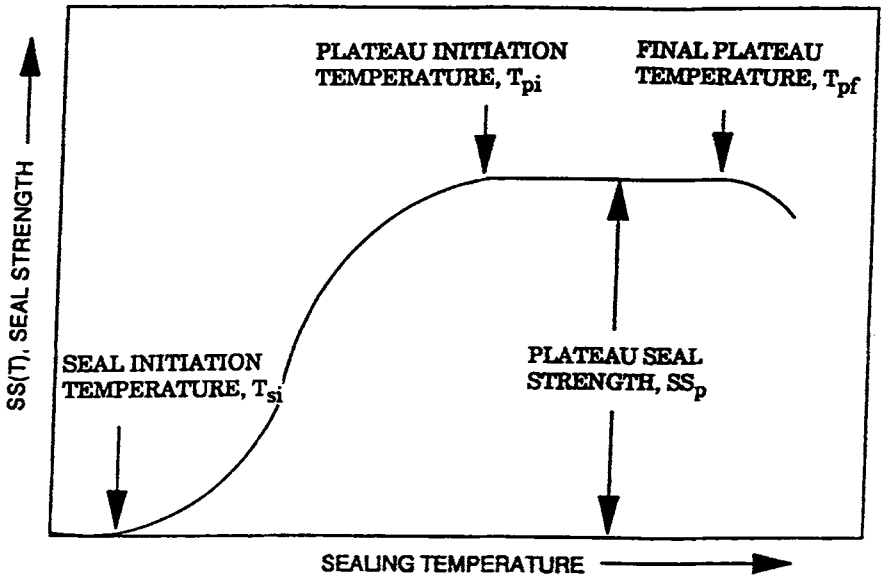

Figure 1 General heat sealing curve, $SS(T)$, relating sealing temperature and seal strength for semicrystalline polymers.

ond or less. Given sufficient time, polymer-chain segments from opposite sides of the interface may diffuse across the interface and create molecular entanglements between polymer molecules in the interfacial zone. Subsequently, cooling and crystallization occurs, yielding a heat-sealed joint. The relative importance of wetting, i.e., increased area of contacting, vis-à-vis entanglement in forming a strong joint is presently controversial.[6]

Previous investigators have noted that a crystalline polymer should be melted in order to form a strong heat seal,[4] but quantitative relationships between melting characteristics and features of the generic seal strength vs. platen temperature plot, $SS(T)$, shown in Figure 1, have not been reported. The $SS(T)$ locus shown in Figure 1 can be approximately described by several quantities illustrated in the figure: (1) the seal initiation temperature, T_{si}, the temperature at which a measurable but low level of seal strength is achieved; (2) the plateau initiation temperature, T_{pi}, the temperature where the plateau region begins; (3) the final plateau temperature, T_{pf}, the temperature where seal strength begins to drop off rapidly and extensive seal distortion sets in; and (4) the plateau seal strength, SS_p. The melting distribution of a crystalline polymer is a plot of weight fraction of the amorphous phase, $f_a(T)$, as a function of temperature, as schematically

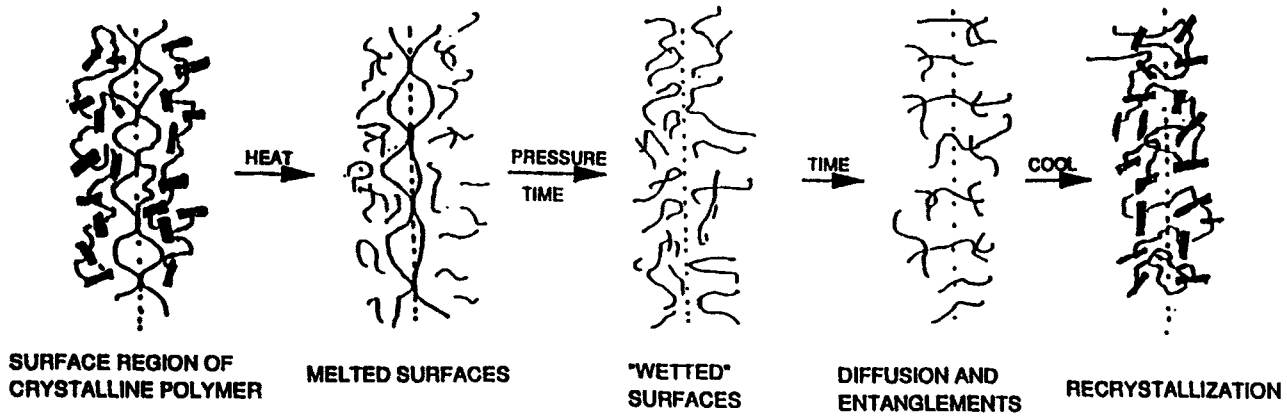

Figure 2 Postulated molecular processes involved in heat sealing of semicrystalline polymer films.

illustrated in Figure 3. Here T_{mf} is the final melting point of the film, i.e., the temperature where $f_a(T)$ becomes equal to one; and $f_a(20)$ is the fraction of the amorphous phase at room temperature: 20°C.

In the work reported here we, examine quantitative relationships between the heat-sealing curve, $SS(T)$, and the melting distribution curve, $f_a(T)$, for numerous, different polyolefins in the form of monolayer film. Our results show that many features of the heat-sealing curve are determined mainly by the melting distribution curve of the polymer film.

EXPERIMENTAL

Polymers

The polymers used in this investigation are listed in Table I. These include polyethylenes of various types, including high density polyethylene (HDPE), i.e., polyethylenes having densities greater than 0.94 g/cc; linear low-density polyethylenes (LLDPE), i.e., poly(ethylene-*co*-α-olefin)s having densities between 0.90 and 0.94 g/cc; very low density polyethylenes (VLDPE), i.e., poly(ethylene-*co*-α-olefin)s having densities less than 0.90 g/cc; and polymers containing long branches obtained by free-radical polymerization at high pressure such as LDPE, poly(ethylene-*co*-vinyl acetate) (EVA), and poly(ethylene-*co*-acrylic acid) (EAA). Ionomers of EAAs, isotactic polypropylene (iPP), and isotactic poly(propylene-*co*-ethylene) (RCP) were also examined. These polymers contained no additives other than low concentrations (roughly 100 ppm) of antioxidants. Antioxidants at these low concentration levels had no measurable effect on heat-sealing behavior. Characterization data, i.e., density by ASTM D1585, melt index (MI) of polyethylenes by ASTM D1238 Condition E, melt flow rate (MFR) of iPPs and RCPs by ASTM D1238 Condition L, and molecular weight data by size exclusion chromatography (SEC) for the polymers are listed in Table I. Molecular weight information for LDPEs, polymers that contain long-chain branches, were determined by SEC with a light-scattering detector. Blends of various polyethylenes were made by melt-mixing weighed quantities of the constituents in a twin screw extruder.

Films

Polymers were converted to monolayer films, typically 50 μm thick, by conventional film blowing or casting processes. Blown films were made on a 38.1 mm extruder screw diameter blown film line at 4:1 blow up ratio, whereas cast films were made on a 25.4 mm extruder screw diameter cast film line. Films are listed in Table II. Force vs. elongation curves at room temperature were obtained on films

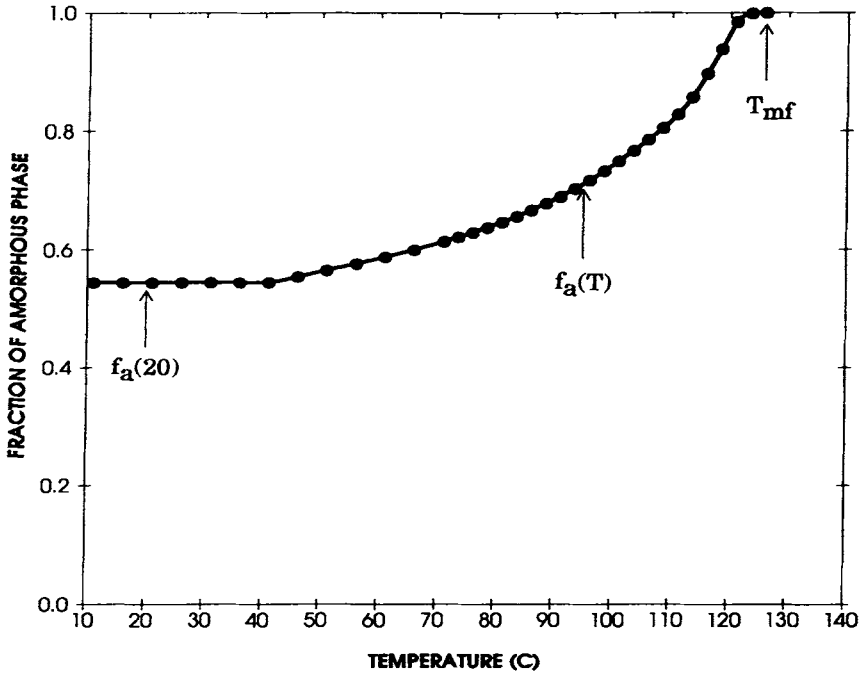

Figure 3 Schematic illustration of melting distribution, $f_a(T)$, of a semicrystalline polymer.

Table I Description of Polyolefins Used for the Study

Polymer Designation	Description	Density (g/cc)	MI/MFR (g/10 min)	$M_w \times 10^{-3}$	$M_n \times 10^{-3}$
1	LLDPE	0.903	0.49	145	69
2	LLDPE	0.903	1.1	112	52
3	LLDPE	0.902	2.2	97	44
4	LLDPE	0.902	3.3	85	40
5	LLDPE	0.907	110	35	13
6	LLDPE	0.910	1.8	80	38
7	LLDPE	0.905	4.2	96	45
8	LLDPE	0.915	4.4	84	41
9	LLDPE blends	0.907	3.7	88	19
10	LLDPE blends	0.910	5.1	81	23
11	LLDPE blends	0.909	3.9	81	19
12	LLDPE blends	0.907	5.4	79	19
13	LLDPE blends	0.910	3.5	79	20
14	LLDPE blends	0.909	3.9	86	17
15	LLDPE blends	0.905	5.0	80	17
16	LLDPE	0.917	1.0	109	31
17	LLDPE	0.911	2.2	106	29
18	LLDPE	0.921	1.0		
19	LLDPE	0.927	1.0	96	25
20	HDPE	0.949	0.04	297	10
21	HDPE	0.944	0.03	316	12
22	LDPE	0.922	2.0		
23	LDPE	0.918	2.0	218	111
24	EVA (2% VA)	0.92	0.32		
25	LDPE	0.918	0.25	211	94
26	LDPE	0.919	0.35	456	107
27	LDPE	0.919	0.75		
28	LDPE	0.926	0.75	165	92
29	LDPE	0.919	2.3	140	72
30	EVA (9% VA)	0.929	2.0		
31	EAA (11% AA)	0.921	8.0		
32	EAA (Zn^{2+})	0.95	2.5		
33	EAA (Na^{+})	0.948	1.0		
34	PP		8.0		
35	PP		7.0		
36	PP		6.0	167	33
37	RCP (5% C_2^{2-})		5.0	172	32
38	RCP (5% C_2^{2-})		5.0		
39	RCP (5% C_2^{2-})		5.0		
40	VLDPE	0.88	8.0	77	35
41	VLDPE	0.891	2.0	89	40
42	VLDPE	0.883	2.0	85	41

that had aged at least 24 hours after forming the films. Mechanical property data derived from the force-elongation curves with the force applied in the machine direction are also listed in the table. Reported values are the average of six or more measurements. All films had a well-defined maximum in the force vs elongation curve, and the maximum in the curve was taken to be the yield point.

Melting distributions for films aged at room temperature for at least 7 days were obtained with a DuPont 912 DSC at 10°C/min scan rate starting at −40°C. To measure the heat of fusion, a base line must be drawn between the points where melting begins and ends, but the beginning of melting is often poorly defined for polymers having a wide melting distribution. This difficulty is minimized for most

Table II Details on the Film Properties

Polymer Designation	Conversion Process Blown/Cast	Film Thickness (μm)	Yield Stress (N/cm^2)	Elongation at Yield (%)	Ultimate Tensile Stress (N/cm^2)	Elongation at Break (%)
1	Cast	50	549	11	2944	485
2	Cast	50	544	9.7	3378	608
3	Cast	50	522	11.2	4014	620
4	Cast	50	512	9.4	2677	671
5	Cast	50	465	8.8	668	635
6	Blown	50	552	8.2	4652	698
7	Cast	44	492	9.8	3773	628
8	Blown	50	688	9.4	4487	648
9	Cast	44	534	10.2	3202	606
10	Cast	40	463	10.5	3476	575
11	Cast	39	528	9.9	3785	598
12	Cast	46	472	8.2	3971	794
13	Cast	36	850	10.9	3409	586
14	Cast	41	594	8.9	3216	652
15	Cast	38	623	10.4	3855	628
16	Blown	50	869	8.2	3169	698
17	Blown	50	750	10.0	3044	657
18	Cast	50	961	8.6	3666	622
19	Blown	50	1338	10.4	3291	586
20	Blown	55	2831	6.2	5496	527
21	Blown	56	2476	7.0	5431	513
22	Blown	50	1076	8.2	2091	279
23	Blown	50	845	7.9	2351	321
24	Blown	50	1029	8.7	2609	309
25	Blown	50	931	8.8	2652	368
26	Blown	50	971	9.7	2926	387
27	Blown	50	1062	10.1	3004	295
28	Blown	50	876	8.5	2287	475
29	Blown	50	928	7.9	2467	315
30	Blown	50	579	8.9	2730	379
31	Blown	50	829	10.5	2875	426
32	Blown	50	1186	9.4	3592	296
33	Blown	50	1737	10.5	3356	286
34	Cast	38	1643	8.6	6224	637
35	Cast	38	1886	9.4	5917	674
36	Cast	38	2213	9.3	5693	564
37	Cast	38	1196	8.6	5313	407
38	Cast	38	1393	10.1	5623	382
39	Cast	38	1241	9.6	5742	439
40	Cast	50	309	10.9	1869	439
41	Cast	50	357	9.9	2117	487
42	Cast	50	341	10.7	1976	429

of the polymers examined here because the onset of melting of aged films was clearly defined and usually set in slightly above room temperature. The heat of fusion of the film sample, ΔH_S, was obtained from the total area under the melting endotherm and comparing it with that of an indium standard. The fraction of the amorphous phase at room temperature, $f_a(20)$, was calculated from the relation

$$f_a(20) = 1 - \left(\frac{\Delta H_S}{\Delta H_U}\right)$$

where ΔH_S is the heat of fusion of the sample, and ΔH_U, the heat of fusion for a 100% crystalline sample, i.e., 70 cal/g for polyethylene[7] and 51 cal/g for polypropylene.[8] The $f_a(T)$ melting distribution is obtained from the equation

$$f_a(T) = f_a(20) + \left[\left(\frac{\Delta H_{Ti}}{\Delta H_S}\right) \times \{1 - f_a(20)\}\right]$$

where, $f_a(T)$ is the amorphous fraction as a function of temperature, ΔH_{Ti}, the cumulative heat of fusion at temperature Ti, and $f_a(20)$, the room temperature fraction of the amorphous phase of the sample. The repeatability of $f_a(T)$ is about 2–3% (absolute) and the precision of T_{mf} is about 1°C.

The $f_a(20)$, the amorphous fraction at room temperature, of films was also determined from density measurements by the density gradient method. The fraction of the amorphous phase was calculated by the method of Chiang and Flory using 1.000 g/cm^{-3} and 0.853 g/cm^{-3} for the densities of the crystalline and amorphous phase, respectively.[9]

Dynamic mechanical properties in tension of selected films were determined using a DuPont 983 DMA using horizontal thin-film clamps. Specimens were heated at 2°C /min from 25 to 180°C, and measurements were made at a constant 1.6 Hz test frequency.

Method for Making and Testing Heat Seals

Methods for making and testing heat seals were identical to those described in Ref. 5. All seals were made by sealing a film to an identical film between two platens set to the same temperature. Platen dwell time and platen pressure were held constant at 1.0 s and 50 N/cm^2, respectively, while the platen temperature was varied. This dwell time is sufficiently long for the interfacial temperature to approach the platen temperature to within about 1°C under our sealing conditions.[5] That is, the maximum interfacial temperature achieved during heat sealing in our experiments virtually equals the platen temperature.

Plots of seal strength against platen temperature were similar but not identical to the schematic plot shown in Figure 1. Values characterizing the seal strength curve, i.e., SS_p, T_{si}, and T_{pi}, are listed in Table III. Some polymers showed a weak maximum at the beginning of the plateau region and the maximum value of the seal strength was then identified as the value of SS_p. T_{si} is defined as the temperature at which seal strength equals 0.7 N/cm, and it was reproducible to within about 2°C. Except for ionomers, all the polymers examined in this work failed in the plateau region by tearing of a leg of the test piece rather than by peeling of the two films. For these polymers, the value of T_{pi} was identified as the lowest temperature at which tearing mode failure occurred, and it was reproducible to within about 2°C. T_{pi} for ionomers was less precisely defined and was reproducible within about 5°C. Data obtained from the melting distribution curves of the corresponding films are alo listed in Table III. These include $f_a(20)$ obtained by both DSC and density measurements, the fraction of the amorphous polymer at the seal initiation temperature, $f_a(T_{si})$, and the final melting point of the film, T_{mf}.

RESULTS AND DISCUSSION

The postulated heat-sealing model illustrated in Figure 2 draws attention to the importance of melting of the semicrystalline polymer in the heat sealing-process. Thus, melting at the interface is necessary to bring two films into Van der Waals contact over a significant fraction of the apparent interfacial area. Additionally, in this view, formation of a strong joint requires that chain segments from opposite sides of the boundary diffuse over a distance of the order of 100 Å so that entanglements in the interfacial zone can occur.

In the discussion below, we examine the correspondence between melting distribution and heat-seal properties. We address in sequence (1) the seal initiation temperature, (2) the transition region between the seal initiation temperature and the initial plateau temperature, (3) the initial plateau temperature, and (4) the magnitude of the plateau seal strength. Our results show that the key features of the seal strength vs. temperature curve, $SS(T)$, can be quite accurately correlated with the melting distribution, $f_a(T)$, and the yield strength, σy, of the film that was sealed.

Seal Initiation Temperature, Transition Region, and Plateau Initial Temperature

Seal Initiation Temperature

Seal strength vs. platen temperature curves for representative polyethylenes covering a wide range of the room-temperature fraction of the amorphous phase are given in Figure 4. Seal initiation temperatures, plateau initiation temperatures, and plateau seal strengths differ widely for these materials, but the curves have shapes similar to that of the idealized $SS(T)$ curve shown in Figure 1. Melting distributions for corresponding films are shown in Figure 5. Compaison of Figures 4 and 5 for corresponding materials shows substantial similarities between the two figures. This comparison suggests that the frac-

Table III Heat-sealing Features

Polymer Designation	f_a (20)/Density	f_a (20)/DSC	f_a (T_{si})	T_{si} (°C)	T_{pi} (°C)	T_{mf} (°C)	SS_p (N/cm)	Failure Mode on the Plateau
1	64	66	78	92	120	121	5.0	Tearing
2	63	65	77	92	120	122	4.9	Tearing
3	64	64	77	87	120	122	5.9	Tearing
4	64	67	76	85	110	112	5.7	Tearing
5	60	59	81	83	120	121	3.1	Tearing
6	58	62	75	82	120	122	6.2	Tearing
7	62	64	77	84	120	121	5.9	Tearing
8	55	58	76	91	125	125	6.4	Tearing
9	61	64	77	86	117	121	5.3	Tearing
10	58	61	75	90	125	126	5.4	Tearing
11	59	62	73	80	122	124	5.8	Tearing
12	60	62	73	84	120	125	4.8	Tearing
13	58	62	75	105	131	133	7.5	Tearing
14	59	61	74	87	122	124	6.2	Tearing
15	62	64	76	85	125	125	6.5	Tearing
16	53	53	76	105	125	125	6.1	Tearing
17	58	61	77	95	126	126	5.7	Tearing
18	54	59	79	107	125	126	7.9	Tearing
19	47	49	78	116	132	133	8.5	Tearing
20	31	33	73	126	138	138	13.5	Tearing
21	35	38	71	125	135	135	12.8	Tearing
22	50	53	74	105	120	121	8.0	Tearing
23	53	55	79	101	115	116	6.7	Tearing
24	51	56	82	100	122	123	7.8	Tearing
25	54	57	74	98	120	121	7.5	Tearing
26	52	52	100	145	165	122	8.0	Tearing
27	53	52	78	102	118	119	6.4	Tearing
28	53	52	75	95	124	124	7.5	Tearing
29	53	52	81	100	118	118	7.4	Tearing
30		62		90	105	106	4.6	Tearing
31		73		80	105	106	6.6	Tearing
32		77.0		85	102.5	102.5	8.4	Peeling
33		77.0		85	102.5	102.5	8.8	Peeling
34		54	59	135	165	167	12.8	Tearing
35		55	60.1	140	165	168	13.3	Tearing
36		56	63.8	148	165	167	15.7	Tearing
37		76	76	120	145	145	6.9	Tearing
38		70	73	120	145	145	8.9	Tearing
39		70	78	120	147	147	10.2	Tearing
40		80	83	50	98	103	3.2	Tearing
41		80	85	53	100	105	4.0	Tearing
42		78	86	60	100	105	3.	Tearing

f_a (T_{si}) = amorphous content at seal initiation temperature; T_{si} = seal initiation temperature; T_{pi} = plateau initiation temperature; T_{mf} = final melting temperature; and SS_p = plateau seal strength.

tion of the amorphous phase at the sealing temperature strongly influences seal strength. The importance of f_a at the sealing temperature for representative films is further illustrated by Figure 6, which is a plot of normalized seal strength vs. the fraction of amorphous phase at the sealing temperature obtained by cross-plotting $SS(T)$ and $f_a(T)$ data. Such a plot of normalized seal strength, i.e., seal strength divided by the plateau seal strength vs. f_a superimposes data from the various polymers to a rough approximation. This indicates that the normalized seal strength for these films is largely determined by the fraction of the amorphous phase at the sealing temperature.

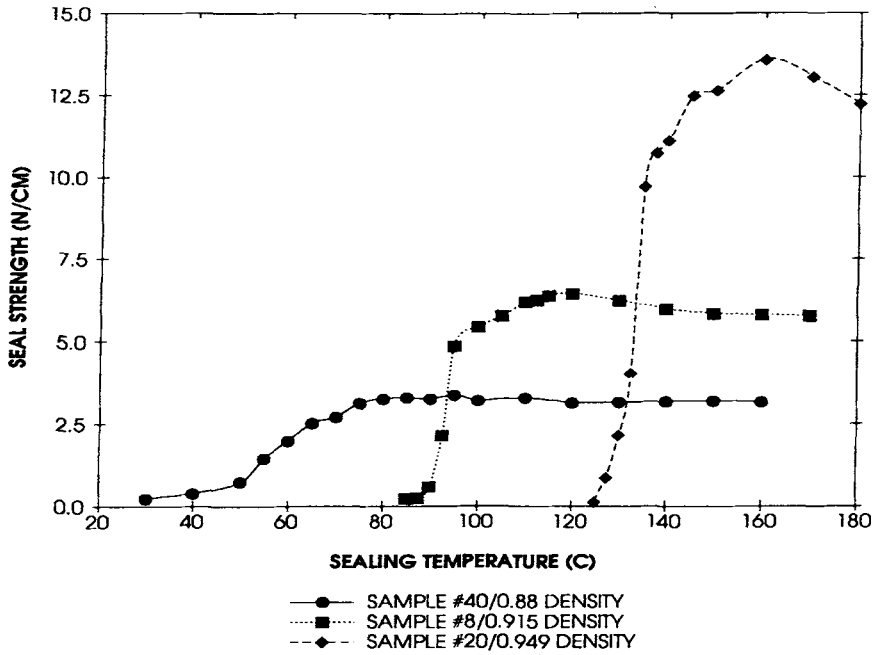

Figure 4 Seal strength vs. sealing temperature curves of various polyethylenes, $SS(T)$.

Figure 6 shows that the initial seal temperature of these polyethylene films, T_{si}, is achieved only after f_a has increased to a high level. The magnitude of f_a at the seal initiation temperature is further addressed in Figure 7, where $f_a(T_{si})$ is plotted against T_{si} for all polymers for which data are available. Filled points in this graph denote ca. 30 polyethylene polymers. Excluding an anomalous point given by Sample 26, the seal initiation temperature for the polyethylenes is approximately constant at 77%, with a standard deviation of 2.9% The sealing behavior of Sample 26 is discussed separately below.

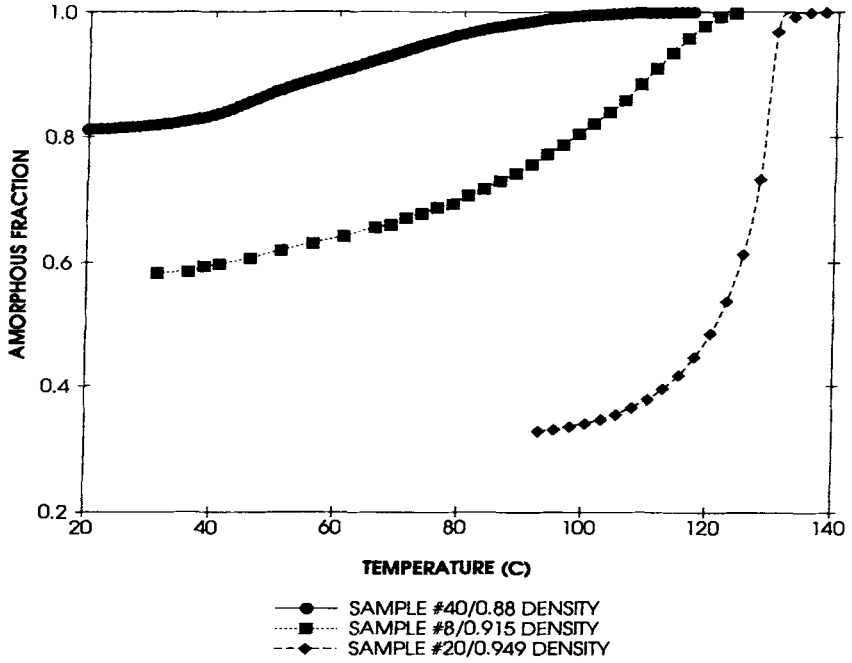

Figure 5 Melting distribution, $f_a(T)$, of various polyethylenes.

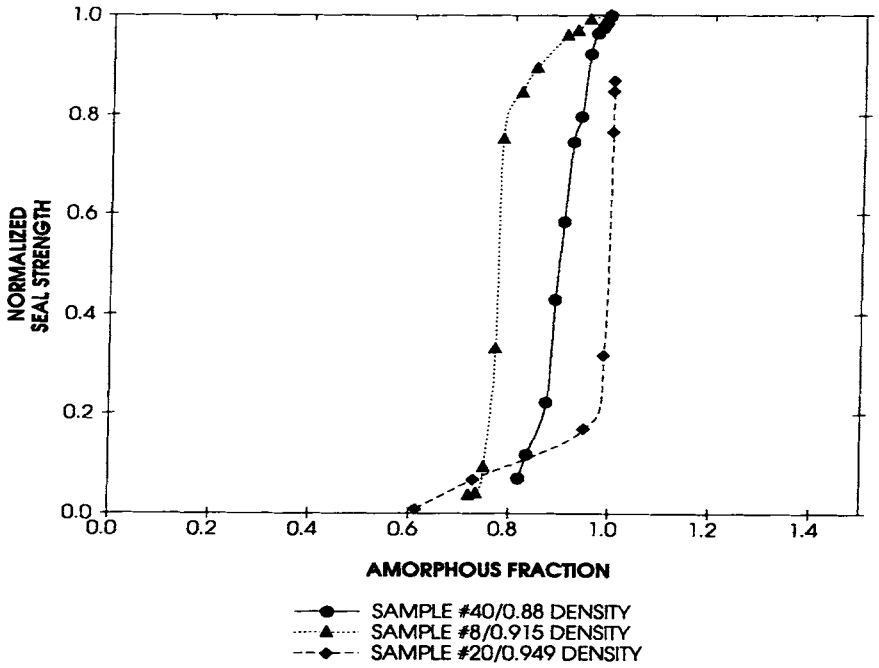

Figure 6 Normalized seal strength vs. sealing temperature for polyethylenes.

Thus, seal initiation for polyethylenes occurs at a nearly constant, high value of f_a equal to about 77%. However, as shown by the open points in Figure 7, the few homopolypropylenes that have been examined have lower f_a values at seal initiation, ~ 60%.

Why is the fraction of amorphous phase nearly constant at the seal initiation temperature for polyethylenes? To rationalize this observation, we have considered the following argument: It is well established that the fraction of the amorphous phase strongly influences the magnitude of the modulus

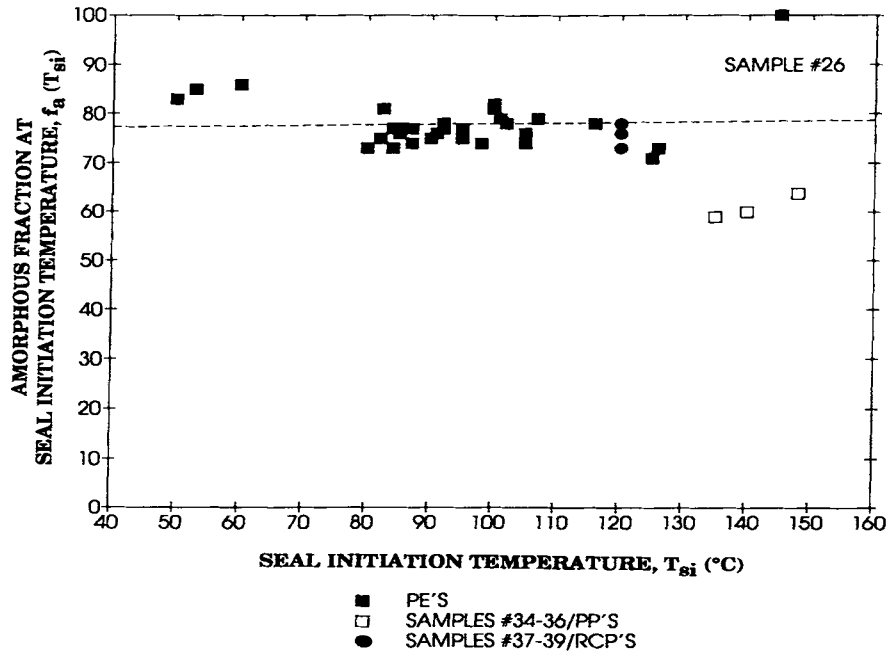

Figure 7 Seal initiation temperature, T_{si}, vs. fraction of amorphous phase at seal initiation temperature, $f_a(T_{si})$, for polyolefins.

of polyethylenes.[10] The constant f_a criterion could therefore conceivably reflect a more general constant modulus criterion for seal initiation that might apply to all semicrystalline polymers, not just polyethylenes. Such a hypothesis is analogous to the Dahlquist criterion for pressure sensitive adhesives.[11] According to the Dahlquist criterion, the modulus of a pressure-sensitive adhesive should be less than a critical value, ca. 3×10^6 dynes/cm^2, so that even a modest applied pressure brings the adhesive into extensive contact with a rigid, microscopically uneven substrate. To test this postulate, the tensile storage modulus of films was measured by dynamic mechanical measurements from room temperature to the final melting point for various polyethylenes and polypropylenes. Table IV shows tensile storage modulus values at the seal initiation temperature for these materials. Values fall into a narrow range from 4 to 11 $\times 10^7$ dynes/cm^2 except for HDPE, whose storage modulus at the seal initiation temperature is well outside this range; 32×10^7 dynes/cm^2. Such a discrepancy might be attributed to annealing affects or to possible measurement errors caused by the strong dependence of modulus on temperature for HDPE at high temperatures. The possible existence of a constant storage modulus criterion for seal initiation is therefore presently uncertain.

In summary, these data support the conclusion that seal initiation for polyethylenes occurs at nearly constant f_a equal to about 77%. However, this value of f_a does not appear to be a general criterion that is applicable to other types of polymers. The question of the possible constancy of the storage modulus at the seal initiation temperature is presently open and requires further investigation.

Transition Region

As shown in Figure 6 for various polyethylene films, seal strength increases as sealing temperature increases and as f_a increases from ca. 0.77 to 1.00. The normalized $SS(f_a)$ data are similar but not identical for the various films in the transition region. The cause of these deviations from more exact superposition will be addressed in a future paper.

Plateau Initial Temperature

The temperature where the plateau begins corresponds closely to the final melting point of the polymer film, i.e., to the temperature where f_a becomes equal to one. This is shown by Figure 8, where the T_{pi} is plotted against T_{mf} for all films for which data are available. The straight line in this figure is the locus $T_{pi} = T_{mf}$, and all points except that of the anomalous Sample 26 fall on this locus within the experimental error of the T_{pi} measurement, ca. 2°C.

Plateau Seal Strength

The magnitude of the plateau seal strength is determined by the yield stress, σ_y, as illustrated for various polymers in Figure 9. The correlation coefficient of SS_p and σ_y for 36 polyethylenes is .89. Ionomers fall closely onto the curve defined by the polyethylenes, whereas homopolypropylenes deviate moderately therefrom. In contrast to the close correlation of plateau seal strength with yield strength, tensile strength at break, σ_b, correlated poorly with plateau seal strength (correlation coefficient equal to .27 for 36 samples).

Why does the magnitude of the plateau seal strength correlate well with σ_y and poorly with σ_b?

Table IV Storage Modulus at Seal Initiation Temperature on Films

Polymer Designation	Sample Description	Seal Initiation Temperature (°C)	Storage Modulus at Seal Initiation Temperature (dynes/cm^2) $\times 10^{-7}$
20	HDPE	126	32
13	LLDPE	105	11
17	LLDPE	95	9.2
25	LLDPE	98	9.3
39	RCP	120	5.0
36	PP	148	10.7
14	LLDPE	87	10.1
44	LLDPE	85	8.8
16	LLDPE	105	3.9
37	RCP	120	8.5

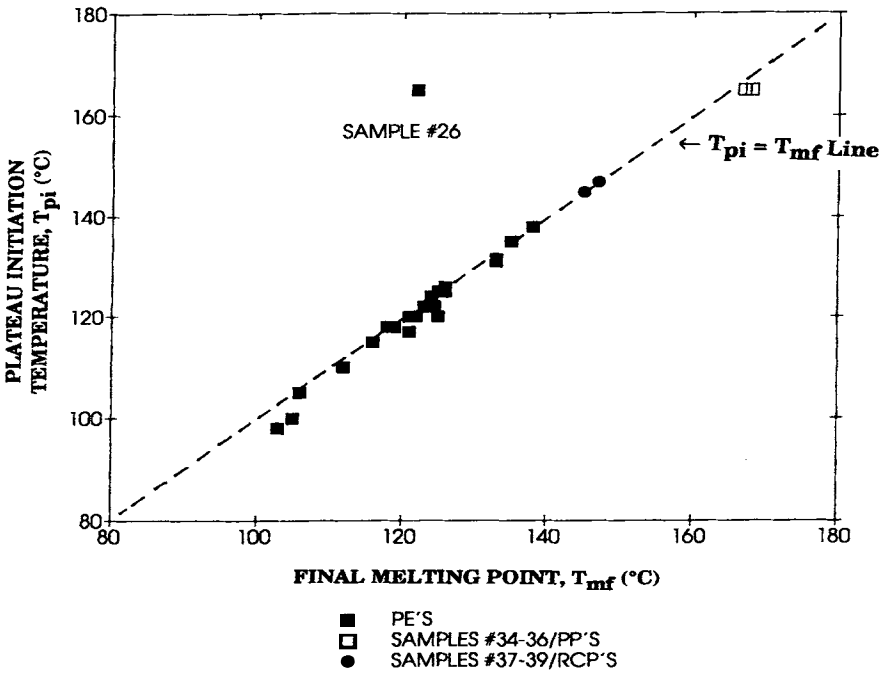

Figure 8 Plateau initiation temperature, T_{pi}, vs. final melting point, T_{mf}, for polyethylenes.

As noted in Ref. 1, seal strength is defined to be the maximum value of the force/width vs. elongation curve of the test piece. In our study, failure in the plateau region occurred by the following sequence of events: (1) the film yielded at a point close to the seal edge, (2) the yielded region propagated along the legs of the test piece until it reached the edge of the seal, i.e., at the point where the two pieces of

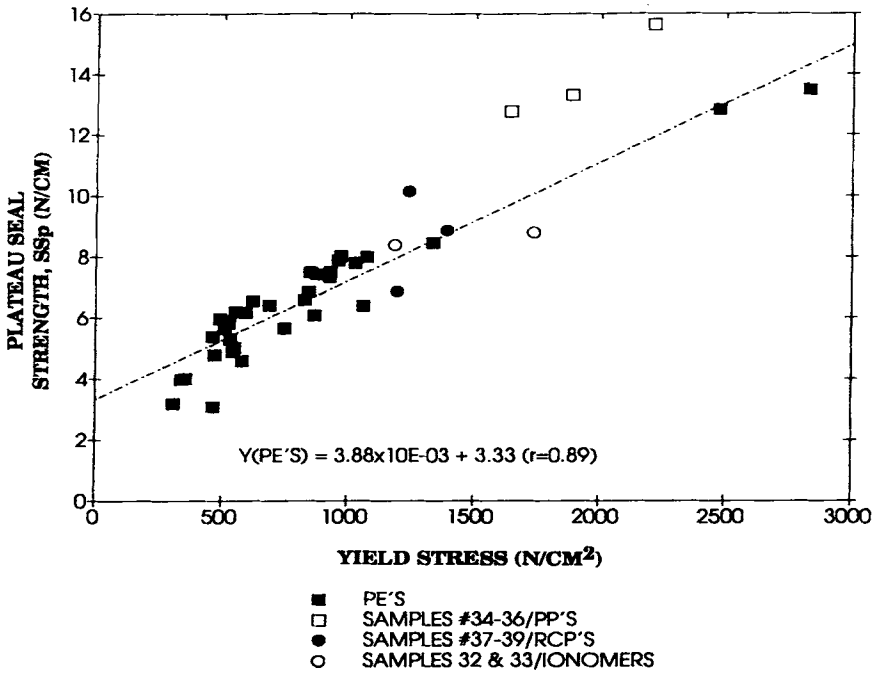

Figure 9 Plateau seal strength, SS_p, vs. yield stress, σ_y, of polyolefins.

film joined, and (3) the leg of the test piece tore off at the edge of the seal (tearing failure, in the case of polyolefins) or the film interface debonded (peeling failure, in the case of ionomers). Seal strength equals σ_y if no strain hardening occurs during the test. If a modest degree of strain hardening occurs, then seal strength modestly exceeds σ_y and if extensive strain hardening occurred, then seal strength could conceivably approach σ_b. The close correlation between the seal strength and σ_y indicates that little strain hardening occurs during the seal test for these samples.

Yield stress of polyethylenes correlates closely with the fraction of the amorphous phase of such polymers,[10] so seal strength in the plateau region of polyethylenes should also correlate with the fraction of amorphous phase at the seal test temperature, i.e., 20°C. Figure 10 is a plot of SS_p vs. $f_a(20)$ for polyethylenes and ionomers derived from poly(ethylene-*co*-acrylic acid). The .7 correlation coefficient of SS_p and f_a is not high, partly because the precision of measuring f_a by DSC is not high, ca. 3% (absolute). As shown in the figure, ionomers have a higher plateau seal strength than that of polyethylenes having a comparable amorphous content. This is attributed to the domain structure of ionomers,[12] which increases their yield stress to higher levels than that of polyethylenes having the same fraction of the amorphous phase.[12,13]

Plateau Final Temperature

Factors that affect the plateau final temperature, T_{pf}, were not extensively examined because of poor precision in defining this temperature and because practical sealing operations are usually conducted at much lower temperatures.

Anomalous Sealing Behavior for Sample 26

As noted above, the heat sealing behavior of Sample 26, an LDPE made by the free-radical-initiated polymerization of ethylene at high pressures, is anomalous. In contrast to all other polymers examined, the initial seal temperature and the plateau seal temperature of this sample, 145°C and 165°C, respectively, are far above the final melting point of the polymer: 122°C. Contamination of a polymer with another incompatible polymer can cause large deviations from the correlations pesented in this report, but no contaminants were detected in this sample.

Polyethylenes made by free-radical processes contain long-chain branches, and it might be proposed that extensive long-chain branching and/or very high molecular weight might be the cause of the anomalous heat-sealing behavior of LD142. The weight-average molecular weight of Sample 26, i.e., 460,000, is indeed substantially greater than that of

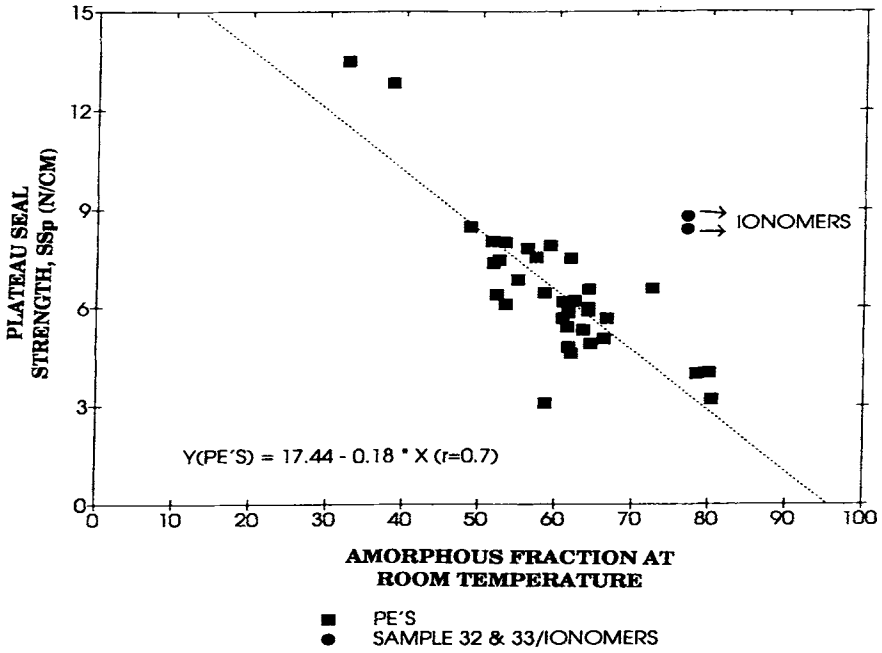

Figure 10 Plateau seal strength, SS_p, vs. fraction of amorphous phase at room temperature, $f_a(20)$, for polyethylenes and ionomers.

any other polymer included in this work. We speculatively propose that this polymer has extensive long-chain branching and high molecular weight and that these factors inhibit wetting and/or the formation of entanglements in the interface.

Comparison of Heat-seal Properties of Polyethylenes and Ionomers

In practical heat-sealing operations, it is frequently desirable to use a film that gives a high plateau seal strength at a low plateau initial temperature. However, as illustrated schematically in Figure 11(A), this combination of properties is difficult to achieve with nonionomeric polyethylenes. HDPE, for example, has a high plateau seal strength but it has a high plateau initial temperature, T_{pi}. T_{pi} can be reduced by introducing a comonomer to reduce the final melting point of the polymr. However, introducing a comonomer such as butene or acrylic acid causes an increase in the fraction of the amorphous phase at room temperature, a decrease in yield stress, and a consequent decrease in the magnitude of the plateau seal strength.

An ionomer and its precursor, e.g., poly(ethylene-*co*-acrylic acid) have very similar melting distributions,[11] so the seal initiation temperature and the plateau initiation temperature for these two materials are similar, as illustrated schematically in Figure 11(B). However, the yield stress of an ionomer is substantially greater than that of its acidic precursor[13], and the ionomer therefore has a substantially greater plateau seal strength than that of its precursor. Ionomers therefore provide the low-heat sealing temperatures characteristic of ethylene copolymers having high comonomer content while maintaining higher levels of plateau seal strength.

CONCLUSIONS

Many features of the apparent seal strength vs. platen temperature curve for semicrystalline polyolefins are determined largely by the melting distribution of the polymer and the yield strength of the polymer. As illustrated in the summary (Figure 12),

1. The seal initiation temperature, T_{si}, for polyethylenes occurs when the fraction of the amorphous phase at the sealing temperature increases to ca. 77%. Seal initiation for other

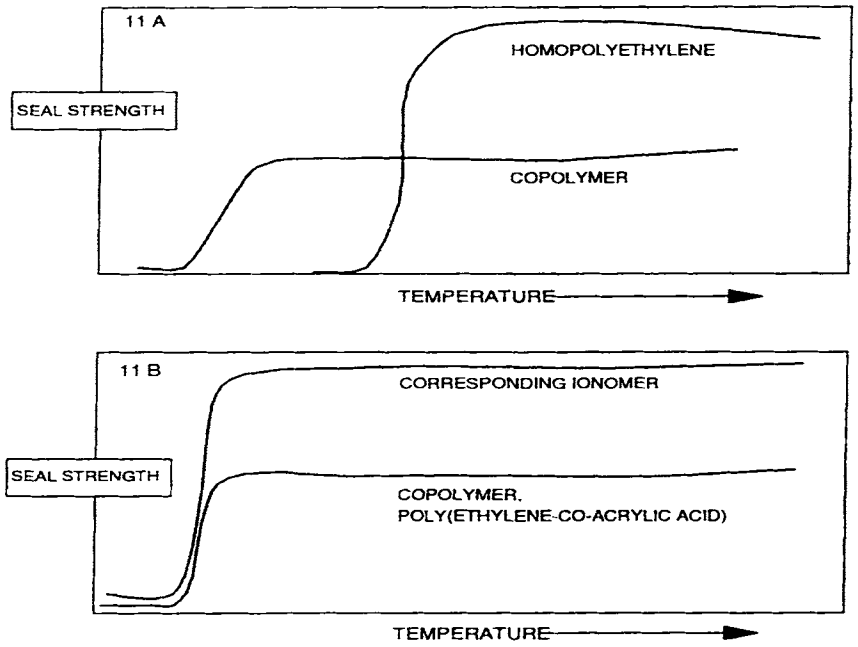

Figure 11 Schematic illustration of lowering of sealing temperature of polyethylene by introducing comonomer, with attendant decrease in seal strength (A); schematic comparison of heat sealing curves of a poly(ethylene-*co*-acrylic acid) and ionomer showing similarity of seal initiation and plateau initiation temperatures of the two polymers but higher seal strength of the ionomer.

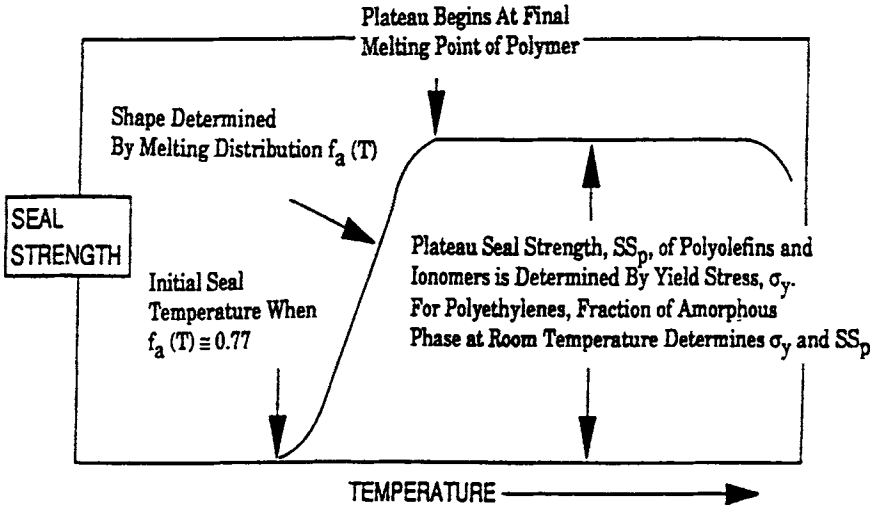

Figure 12 Summary of effect of melting distribution on heat sealing curve of polyolefins and ionomers.

polyolefins does not adhere closely to this constant f_a criterion. The question of whether a constant modulus criterion applies at the initial seal temperature requires further investigation.

2. The fraction of the amorphous phase at the sealing temperature strongly affects the shape of the sealing curve in the transition zone between the initial seal temperature and the initial plateau temperature. To a rough approximation, plots of seal strength vs. the fraction of the amorphous phase at the sealing temperature for various polyethylenes superimpose.
3. The initial plateau temperature corresponds closely to the final melting point of the polymer film for all polyolefins and ionomers examined.
4. The magnitude of the plateau seal strength is determined largely by the yield stress of the polymer film and not by tensile stress. The yield stress of polyethylenes is a function of the fraction of the amorphous phase, so the plateau seal strength of polyethylenes also correlates with the fraction of the amorphous phase at room temperature. The heat-seal curve of polyethylenes can therefore be predicted with useful accuracy from the DSC thermogram of the polymer.
5. Our results explain why ionomers are desirable heat-sealing polymers. An ionomer has a melting distribution similar to that of its acidic precursor, but it has a higher yield stress because of the ionic domains present in an ionomer. Consequently, an ionomer has a higher plateau seal strength than that of a polyolefin if the comparison is made for polymers having similar sealing temperatures. Conversely, if the comparison is made at the same level of plateau seal strength, then the ionomer has a lower sealing temperature.

In summary, the main features of the heat-sealing curve for polyethylenes can be rather accurately predicted from a DSC melting distribution of the film to be sealed. Melting distributions of semicrystalline polymers are affected by crystallization conditions, so the DSC measurement is preferably made on the film that is to be sealed. In the absence of such a film, a few milligrams of the polymer crystallized in a DSC instrument may be used, but with attendant loss in accuracy of the predicted sealing performance. For other polyolefins and ionomers, where the relationship between the fraction of the amorphous phase and yield strength is less well established than for polyethylenes, the magnitude of plateau seal strength should be estimated from the measured yield strength of the polymer film and not from the percent crystallinity of the film.

Caution should be exercised in applying the above conclusions to polymers whose compositions and molecular weights differ widely from those of the polymers used to establish the above correlations. In our treatment, we have interpreted results solely in terms of bulk properties of films, i.e., melting distribution and yield strength. Interfacial considera-

tions, such as possible partitioning of molecules between bulk and interfacial phases because of molecular weight or compositional variations, the degree of molecular contact between molecules from opposite sides of the interface, the state of entanglement of molecules in the interfacial zone, etc., have been neglected. A more accurate treatment of heat-sealing performance must address such matters.

We are grateful to Keith Jolibois, Becky Cornett, and Beverly Poole for experimental assistance and to Wilfried van Craeynest and Jim Farley for many helpful discussions.

REFERENCES

1. M. G. Dodin, *J. Adhes.* **12**(2), 99 (1981).
2. M. G. Dodin, *Physicochemical Aspects of Polymer Surfaces II*, K. L. Mittal, Ed., Plenum Press, New York 198) pp. 717–736.
3. H. W. Theller, *J. Plast. Film Sheet.*, **5**, 66 (1989).
4. V. K. Stokes, *Polym. Sci. Eng.*, **29**(19), 1310 (1989).
5. P. Meka and F. C. Stehling. *J. Appl. Polym. Sci.*,to appear.
6. M. D. Ellul and A. N. Gent. *J. Polym. Sci.: Polymer Phys. Ed.*, **22**, 1953 (1984).
7. L. Mandelkern, *Crystallization of Polymers*, McGraw-Hill, New York, 1964, p. 119.
8. D. R. Gee and T. P. Melia, *Makromol. Chem.* **132**, 195 (1970).
9. R. Chiang and P. J. Flory, *J. Am. Chem. Soc.*, **83**, 2057 (1961).
10. A. J. Peacock and L. Mandelkern, *J. Polymer Sci.: Part B Polym. Phys.*, **28**, 1917 (1990).
11. C. A. Dahlquist, *Adhesion: Fundamentals and Practice*, Maclaren, London, 1966.
12. W. J. McKnight, W. P. Taggert, and L. McKenna, *J. Polym. Sci. Symp.* **46**, 83 (1974).
13. R. W. Rees, U.S. Pat. 3,264,272 (1966).

Received March 4, 1993
Accepted June 18, 1993